Adhesion Asymmetry in Peeling of Thin Films with Homogeneous Material Properties: A Geometry-Inspired Design Paradigm

Ahmed Ghareeb
Civil and Environmental Engineering, University of Illinois at Urbana-Champaign
2119 Newmark Civil Engineering Lab, 205 N. Mathews Ave, Urbana, IL 61801
ghareeb2@illinois.edu

Ahmed Elbanna[1]
Civil and Environmental Engineering, University of Illinois at Urbana-Champaign
2219 Newmark Civil Engineering Lab, 205 N. Mathews Ave, Urbana, IL 61801
elbanna2@illinois.edu

ABSTRACT

Peeling of thin films is a problem of great interest to scientists and engineers. Here, we study the peeling response of thin films with non-uniform thickness profile attached to a rigid substrate through a planar homogeneous interface. We show both analytically and using finite element analysis that patterning the film thickness may lead to direction-dependent adhesion such that the force required to peel the film in one direction is different from the force required in the other direction, without any change to the film material, the substrate interfacial geometry, or the adhesive material properties. Furthermore, we show that this asymmetry is tunable through modifying the geometric characteristics of the thin film to obtain higher asymmetry ratios than reported previously in the literature. We discuss our findings in the broader context of enhancing interfacial response by modulating the bulk geometric or compositional properties.

Keywords

Interfacial adhesion; Adhesion Asymmetry; Peeling Force;

[1] Corresponding author.

1. INTRODUCTION

Understanding the mechanics of adhesion of thin films to rigid substrates continues to be a topic of extensive research in science and engineering. Films attached to substrates are very common in many engineering and biological systems such as solar panels [1], integrated circuits [2], flexible electronics [3], packing and adhesive tapes [4], coatings [5], and medical tapes [6]. The bonding strength of the interface is usually quantified by the adhesion energy [7], defined as the amount of energy required to create a unit area of fractured surface. In many applications, strong bonding between the film and the substrate is required to ensure system reliability. However, other properties may be desirable such as having asymmetric response when peeling the thin film from one direction versus the other.

Asymmetry in the peeling of thin films is the dependence of peeling force, adhesion energy, or both on the direction or the axis of peeling. Asymmetry may be utilized to achieve reversible control of adhesion, which is the ability to change adhesion strength from weak to strong modes, through changing the direction of peeling. This feature is critical to many existing and potential engineering systems, including but not limited to, climbing robots, medical tapes, and stamps for transfer printing [8].

In the past few decades, extensive research has been conducted to better understand various aspects of the peeling mechanism of thin films in terms of both the adhesion strength and energy [7, 9]. Several studies have focused on improving the bond strength and adhesion energy by changing the mechanical properties of the interface, through the modification of interface topology and roughness, to alter the

conditions of nucleation and propagation of peel front. [10–13]. This pointed to the possible role of adherent or interface heterogeneities in controlling the peeling response and opened new opportunities for utilizing these heterogeneities to improve the adhesion [14–21].

The peeling asymmetry has also been realized through a variety of techniques such as using non-uniform distribution of adhesive strength [22], adding arc patterns on the interface [18], changing the geometry of the interface through adding arrays of tilted microfibrils [23], and adding arrays of nano-fabricated polymer pillars coated with a thin layer of a synthetic polymer [24] inspired by geckos [25]. Other studies included using a duplex attachment pad composed of two geometrically identical wedge shaped blocks with different modulus of elasticity [26], or using shape memory polymer surfaces with geometrically asymmetric micro-wedge arrays for reversible dry adhesives [27]. However, none of these studies have demonstrated the possibility of inducing adhesion asymmetry in the peeling response using solely changes in the thickness of the film.

In this paper, we focus on studying the peeling response of homogeneous thin films, with patterned thickness, from rigid homogeneous substrates. We show using a semi-analytical approach and finite element analysis that varying the film thickness may lead to asymmetry in the peeling response. Furthermore, we show that this asymmetry is tunable and can reach higher values than that reported in several previous studies [18, 22, 27]. We also investigate the dependence of the asymmetry ratio on various model parameters.

2. RESULTS

2.1 Theoretical Prediction for Adhesion Asymmetry in Thin films with Variable Thickness

We follow the analytical procedure developed by Xia et al. [16] for the analysis of adhesion in heterogeneous thin films. **Fig. 1-a** shows a schematic diagram of the non-uniform strip under consideration here. The strip is modeled as an inextensible Euler-Bernoulli beam. This assumption holds for moderate or large peel angles [9]. The strip is discretized into N segments, having the same elastic modulus (E) and Poisson's ratio (ν), but each one has a different thickness (t), and hence different bending rigidity $D_i = EI_i = Ebt_i^3/12(1-\nu^2)$ where I_i is the second moment of area of the i^{th} segment, and b is the strip width. The strip thickness is described by a sawtooth function with thickness varying between t_l and t_h as shown in **Fig. 1-b**.

The strip profile is uniquely described by a function of $\theta(s)$ where θ_i is the angle between the tangent to the strip and the horizontal plane at discretization node i, and s_i is the arc length from the origin point o along the strip to node i. The film is perfectly bonded to the rigid substrate up to the point where $s = s_o = l$, and is being peeled by a force $\boldsymbol{F}$ with peeling angle θ_p. The potential energy of the idealized beam is given by:

$$\varepsilon = \sum_{i=1}^{N} \int_{s_{i-1}}^{s_i} \frac{1}{2} D_i \big(\theta'(s)\big)^2 ds - \int_0^{s_N} F\big(\cos(\theta - \theta_p)\big) - 1) ds - \int_0^l G ds \qquad (1)$$

Where G is the adhesion energy per unit length of the interface between the strip and the substrate. Rate-independent adhesion energy is assumed in this study similar to some prior work [16]. However, the qualitative nature of the results is not expected to

change if rate dependence is assumed as long as inertia effects are dominated by damping forces. We also assume a smooth homogeneous interface and thus the value of G is taken to be spatially constant. Heterogeneities in G, for example due to surface roughness, may lead to adhesion asymmetry on its own [18] and thus we elect not to include it in this study to critically evaluate the role of film geometry alone on the effective adhesion.

The condition of equilibrium of the strip is that the first variations of **Eq. 1** vanishes. As shown in Xia et al. [16] this yields the following relation for the peeling force and the thin film elastic line:

$$F = \frac{D_1 G}{\sum_{i=1}^{N} D_i f(\theta_i, \theta_{i-1})} \tag{2}$$

And

$$\frac{d\theta}{ds} = \frac{\sqrt{2}}{D_k} \sqrt{D_1 G - F\left(\sum_{i=1}^{k-1} D_i f(\theta_i, \theta_{i-1}) + D_k f(\theta, \theta_{k-1})\right)} \tag{3}$$

Where $f(\theta_n, \theta_m) = \cos(\theta_n - \theta_p) - \cos(\theta_m - \theta_p)$. **Eq. 2, 3** are solved numerically to determine the force F and the slope angles $\theta_1 : \theta_N$. The solution scheme and the details of the discretization process are outlined in the methods section.

Since the thickness profile of the strip is sawtooth as shown in **Fig. 1-b**, the normal stresses are redistributed at the locations where the thickness is changing abruptly leading to a smoother transition in the stress profile. The effective thickness $t_{eff.}$ for resisting bending deformation is thus smaller than the local thickness of the strip in these regions and the two thickness measures coincide only after a horizonal

transition distance as shown in **Fig. 1-c**. This horizontal distance is estimated using the finite element model under the same boundary conditions as the theoretical model, i.e. the film is perfectly bonded to the rigid substrate up to the crack front, and is found to be nearly equal to the step change in the thickness. We use the effective thickness profile to calculate the rigidities of segments D_i when numerically integrating **Eq. 2, 3**.

We normalize the peak force F_{peak} with respect to the peeling force of a homogenous strip given by $F_{hom} = G/(1 - cos\theta_p)$ [7]. Furthermore, we follow Xia et al. [16] and introduce the following length scale:

$$\lambda = \sqrt{\frac{D_e}{2G}} \tag{4}$$

Where D_e is the effective rigidity of the strip, and G is the adhesion energy. This length scale represents the length of a strip of stiffness D_e subjected to a moment generated by a force proportional to the adhesion energy G. We will use this length scale to normalize the period p. For a strip with varying thickness, we define the effective rigidity as $D_e = \frac{1}{p}\left(\int_0^p \frac{dx}{D(x)}\right)^{-1}$.

We use the following parameters in the numerical integration of the model unless otherwise stated: Young's modulus E = 1 GPa, and Poisson's ratio υ = 0.35 and fracture energy G= 35 J/m2 [4]. The peeling angle θ_p is kept constant at 90 degrees.

The results of the semi-analytical model are shown in **Fig. 2**. The results in **Fig. 2-a,b** show that peeling force required to advance the peeling front in direction 1 (Forward peeling) is higher than that required for direction 2 (Backward peeling). We

call the ratio between the maximum force in each direction the Asymmetry ratio. For forward peeling, the peel front stops at the location of the sudden increase in the thickness. The force increases till it reaches a peak value, then the peel front propagates with a decrease in force until the peeling front reaches the next sudden increase in thickness. However, for backward peeling, the force increases gradually while the peel front propagates in the direction of increasing thickness. The force then drops as the thickness is abruptly reduced. For both directions, the peak force is higher than that of a homogenous strip. The sudden increase in the normalized peak force in the case of forward propagation is similar to the case of a strip with piecewise thickness, i.e. strip with uniform high thickness segment followed by low thickness segment [16]. However, in the case of piecewise thickness distribution, the peeling behavior is symmetric, and the peak force is the same in both peeling directions.

To verify the predictions of the analytical model, we use the finite element software package ABAQUS [28] to simulate a quasi-static peeling test of a thin film with the same saw tooth profile and model parameters as used in the analytical model. The FEM model is composed of three main parts: (i) a rigid base plate that represents the substrate, (ii) a thin film with varying thickness, and (iii) a zero-thickness cohesive layer joining the film and the substrate to represent the adhesion between the two components. The details of the model setup are included in the methods section.

The length on the interface between crack initiation and total separation defines the cohesive zone length l, which depends on the film thickness and a characteristic length that depends on the bulk material properties and the cohesive zone model parameters [29]. The characteristic length L_{ch} of the cohesive law is given by [30]:

$$L_{ch} = \frac{E\ G_c}{{\sigma_{cr}}^2} \tag{5}$$

Where E is young's modulus of the bulk material, G_c is the cohesive model energy release rate, and σ_{cr} is the critical cohesive stress. This is another important length scale that controls the adhesion response as we will discuss later.

Figure 2-a,b show the normalized force vs the normalized peel front position, whereas **Fig. 2-c,d** show the normalized force vs the normalized vertical peel displacement. The finite element results are plotted along with the theoretical results using the effective thickness. Both the finite element and the theoretical model solutions share the same trend and match well in the middle part of the unit cells as shown in **Fig. 2-a,b** . Some discrepancy exists at the location of sudden change in thickness due to the complicated stress redistribution at this zone. In addition, the finite element normalized force vs peel displacement plots shown in **Fig. 2-c,d** for both the forward and backward propagation show a snap-back effect due to the nature of the displacement controlled loading we adopt in the finite element model which does not allow the tip displacement to decrease. The hatched areas in **Fig. 2-c,d** represent the energy dissipated due to this snap-back instability. The effective energy release rate

calculated from the finite element model for this case is $1.045G_c$ for forward propagation and $1.02G_c$ for Backward propagation.

Figure 2-e,f show the maximum normalized peak force as a function of the normalized period for the theoretical model using the actual thickness, the theoretical model using the effective thickness, and the finite element results for both forward and backward peeling and thickness ratio of 0.5. For forward propagation, the semi-analytical model using the actual thickness is completely off the other two curves. The sudden change in thickness leads to higher peak force than the gradual change. The semi-analytical model using the effective thickness, and the finite element results have good agreement for large normalized periods. However, as the period approaches the value of the bending length scale $(p/\lambda = 1.00)$, the discrepancy increases. Similarly, for backward peeling, the solution for the three models show good agreement at large values of normalized period. Both the semi-analytical model using the effective thickness and the finite element results show non-monotonic dependence of the peak force in the backward peeling direction on the normalized period. This may be attributed to the changes in the slope of the film free surface as follows.

For a similar problem of a tapered cantilever beam with mode I adhesive interfacial fracture, the critical strain energy release rate is given by $G_c = (P^2/2b)\,(dC/da)$ [31] where, G_c is the adhesion energy, P is the critical load, b is the width of the specimen, and dC/da is the compliance rate change with respect to crack length a. For a constant adhesion energy G_c, the relation between the critical load and the compliance rate change with respect to crack length is $P \propto (dC/da)^{-1/2}$. Qiao

et al [32] showed analytically that for a tapered cantilever beam with linearly increasing thickness, dC/da increases with reducing the slope of the tapered beam. Hence, decreasing the slope, through increasing the period length for the same thickness ratio, leads to higher compliance rate change with respect to crack length and hence lower critical load.

2.2 Tunability of the Adhesion Asymmetry

Here, we show using the finite element model results that the adhesion asymmetry is tunable and investigate its dependence on different model parameters including: the thickness ratio, the normalized period, and the adhesive characteristic length.

Figure 3-a shows the relation between the thickness ratio and the normalized peak force for both forward and backward peeling for three different period lengths to the strip maximum thickness ratios p/t_h. Decreasing the ratio between the minimum and maximum thickness leads to an increase in the peak force for both forward and backward peeling. However, the rate of increase is higher for the forward peeling and thus the asymmetry ratio increases as shown in **Fig. 3-b.** As the thickness ratio approaches 1, the peak force for both forward and backward peeling approaches that of a uniform homogenous strip and thus the asymmetry ratio goes to 1 (symmetric behavior).

Figure 3-c shows the relation between the normalized peak force and the normalized period for both forward and backward peeling and two different thickness ratios. For forward peeling, the normalized peak force has a value of 1 as the normalized

period approaches 0, which represent the case of homogenous uniform strip. The normalized peak force increases with increasing the normalized period, approaching a maximum value that depends on the thickness ratio. For backward peeling, the peak force has a value of 1 at small normalized period values. The normalized force increases with increasing the normalized period till it reaches a maximum value that depends on the thickness ratio, then it decreases with increasing the period and asymptotically approach 1. This non-monotonic trend may be explained as follows. As the period becomes small enough, of the order of the thickness difference $(t_h - t_l)$ or smaller, the bending stresses are concentrated in a strip of thickness t_l (i.e. the smaller thickness) and thus the effect of thickness variation decreases and the response approaches that of a strip with uniform thickness. Longer periods enable stresses to be distributed across the full strip thickness, except within the transition length around the step change in thickness, and thus the effect of thickness variation becomes more pronounced. This non-monotonic behavior is not captured by the semi-analytical model using the apparent thickness as the peak force keeps increasing with decreasing the normalized period as shown in **Fig. 2-f**. The semi-analytical model, however, correctly predicts this non-monotonicity when the effective thickness is used.

Since the film thickness is varying in our study, the cohesive zone length changes with the peel front location. To demonstrate the interplay between the properties of the cohesive law and the film variable thickness, we instead use the characteristic length scale L_{ch} since it depends only on the cohesive law parameters and the film material properties. **Fig. 3-e** shows that increasing the cohesive interface characteristic length

L_{ch} relative to the bending length scale λ reduces the effect of thickness variation in the case of forward peeling. When the cohesive zone size increases, the effect of changing the thickness is smoothed leading to homogenous like behavior. Similar results have been recently reported for peeling of thin films with material heterogeneities, where the peel force enhancement due to heterogeneities in the film material properties decreases with increasing the cohesive zone length [33]. **Fig. 3-f** shows that with decreasing L_{ch}/λ, the asymmetry ratio increases and approaches the theoretical estimate for this choice of parameters. The characteristic length may be increased by using adhesives with higher intrinsic adhesion energy or lower intrinsic strength. Thus, the asymmetry may be maximized for interfaces that are intrinsically strong and brittle.

We note that the asymmetry ratios reported in **Fig. 3-b,d** approach a value of 7. This ratio exceeds what has been reported previously in the literature [18, 22, 27] as we will discuss further in the discussion section. The asymmetry ratio may be further increased through tuning the geometric parameters (e.g. by further decreasing the thickness ratio t_l/t_h or increasing the normalized period p/λ).

2.3 The Energetic Underpinning of Adhesion Asymmetry

To gain further insights into the details of adhesion response asymmetry, we investigate the change in strain energy of the strip at steady state peeling for both forward and backward peeling directions. The strip strain energy is normalized by the strain energy of a homogenous strip having a uniform thickness $t = t_h$. **Fig. 4** shows that the strain energy in the strip depends on the peeling direction.

For forward peeling, the strip requires a high force for the peel front to suddenly propagate from the low thickness to high thickness. Hence, the strain energy in the strip increases at this zone then it starts decreasing while the peel front propagates in the direction of decreasing thickness. For backward peeling, the force continues to increase, and the strip gains more energy while the peel front propagates in the direction of increasing thickness. After that, the energy starts decreasing gradually due to the stress redistribution that occurs near the location of the sudden drop in thickness. The results suggest that the peeling force enhancement in the forward peeling direction is due to the rapid variation in the stored elastic energy as the peeling front crosses under segments with different thicknesses.

3. DISCUSSION

The primary result of this paper is that for a thin homogeneous strip adhered to a rigid substrate, patterning the strip thickness leads to asymmetry in the peeling behavior without changing the interface adhesive properties. If compared with a strip having a uniform thickness, a strip with patterned thickness shows enhanced adhesion strength that is higher in one direction than the other. The asymmetry ratio increases with (a) increasing the difference between the thickness at the beginning and the end of the period, (b) increasing the period length with respect to the length scale of bending, and (c) reducing the cohesive zone length to bending length scale ratio.

The asymmetric behavior is attributed to the difference in the strain energy required to peel the strip in the two directions. When the peel front propagates suddenly from low thickness to high thickness zones in forward peeling, the rapid

variation in stored elastic energy leads to significant enhancement in the force. This enhancement is due to high fraction of the external work exerted to increase the stored energy in the strip to bend the suddenly thicker and hence stiffer region. This is similar to the findings of Xia et al [16] on peeling of heterogeneous films with patterned elastic moduli. However, our current work shows that in a film with patterned thickness this mechanism may also lead to adhesion asymmetry. In backward peeling, as the peel front propagates in the direction of increasing thickness, it also requires higher strain energy and hence higher external work and force. The enhancement in the forward propagation is higher than that of the backward propagation leading to asymmetry. The location of the peak force for forward propagation is at the sudden increase in thickness, whereas for the backward propagation is found to be in the fourth quarter of the period.

We have used a semi-analytical model based on inextensible Euler-Bernoulli beam to analyze the peeling problem. The assumption of inextensibility is acceptable for moderate and high peeling angles [9]. However, for soft strips with low peeling angle, the effect of extensibility may become important [9]. One limitation of using one dimensional model in the analytical approach is that we do not allow for adhesion asymmetry in the transverse direction. It is thus implied that the peeling out of plane is uniform and follow the Rivlin model [7]. However, the semi analytical model serves to prove that introducing designed irregularities by patterning the thickness may lead to adhesion enhancement and asymmetry, and the same concept may be applied to

peeling of two-dimensional sheets by patterning the thickness in two orthogonal directions. This will be the focus of a future investigation.

The direction dependency in peeling has been explored in previous studies where the adhesion strength may be made dependent on the axis of the pull or the peeling direction [18, 22–24, 27]. Direction dependency enables changing adhesion strength from weak to strong modes based on peeling direction which could be a desirable feature in many systems, such as climbing robots, medical tapes, and stamps for transfer printing [8]. However, most, if not all, of the previous studies dealing with direction dependency and reversible control of adhesion leverages changes in the geometry of the interface or the material properties of the adhesive layer, or require external factor to stimulate the different peeling modes, such as temperature [34].

In this paper, we propose, for the first time to the best of our knowledge, a simple and efficient way to introduce asymmetry by patterning the thickness of the thin strip for the same bulk material, and interface properties. We have achieved asymmetry ratios close to 7 which exceeds what have been reported previously in the literature. For example, in the work of Xia it el [18], the reported asymmetry ratio using interfacial arc patterns was around 1.5. In Hsueh and Bhattacharya [22], the reported maximum asymmetry ratio through optimizing adhesion strength distribution was around 2.5. In the work of Seok et al [27] using micro-wedge array surface, the reported asymmetry ratio was around 5. However, the studied mechanism in Seok et al [27] requires temperature changes. By controlling parameters such as thickness ratio or the periodicity of the thin film in our design, the asymmetry effect may be further increased.

The geometric parameters to tune asymmetry in our proposed pattern are easily controlled due to the recent advances in manufacturing techniques and 3D printing [35] and thus provide an attractive passive pathway for achieving high adhesion asymmetry ratios in a variety of applications.

An indirect result of the theoretical model is that adhesion asymmetry may be also achieved in a thin film with uniform thickness by using a periodic distribution of elastic modulus gradient along the longitudinal direction. While it is not unexpected that adhesion will be asymmetric in peeling of a film with monotonic gradient in its elastic properties, it is not very clear that this should be the case for periodic variations. This is because in the latter case, the homogenized elastic properties of a unit cell will be direction independent. In particular, a Bloch-wave analysis for the unit cell (not shown here), assuming linear elasticity, yields a symmetric dispersion relation. One value of the theoretical model is that it suggests the asymmetry in adhesion persists even in the case of a film with periodic gradient elasticity in the longitudinal direction. We note, however, that our proposed approach in varying film rigidity through patterning thickness is possibly easier, from a manufacturing perspective, than producing gradients in elastic properties. Furthermore, since rigidity has a linear dependence on the modulus of elasticity but cubic dependence on film thickness, it is possible to obtain large asymmetry ratios from small variations in thickness.

In this work, we focus on the asymmetry of the peak force required to peel a film with patterned thickness, but we note that it is also possible to describe adhesion in terms of the total work required to peel off the film which is given by the area under the

force displacement curve. For low peeling velocities considered in this study, the asymmetry in the peak force was found to be larger than the asymmetry in the peel work. We expect the peel work for both forward and backward peeling to increase with increasing the rate of peeling, even for adhesives with rate-independent adhesion energy. When the peel front propagates under the sudden change in thickness, waves are radiated due to the snap-back effect noticed in the finite element results in **Fig. 2-c,d** and affect the peel work. The peeling rate effect will further increase if the film material or the adhesive properties are rate-dependent. The effect of rate dependence on the asymmetry of both peel force and peel work will be the focus of future work.

This work also highlights the role of stiffness variation in material design particularly related to problems in fracture or adhesion. Heterogeneities in general, through patterning the bulk geometry, introducing voids, introducing patterned cuts, or adding soft or hard inclusion may result in materials with enhanced fracture toughness [36], wave propagation properties [37], negative Poisson's ratio [38], or improved adhesion [38, 39], among other material properties. This opens new pathways in designing and fabricating metamaterials with optimized and enhanced material priorities.

Recently, there has been an increased interest in non-reciprocal behavior in the mechanics and physics communities especially in the context of wave propagation. The possibility of breaking the wave propagation symmetry or obtaining one-way propagation is highly desirable in many technological applications [41]. Although our current work focuses only on the peeling strength, future extensions may find

connections to problems in wave propagation. It will be potentially interesting to investigate the propagation of interfacial waves that may develop during dynamic peeling and whether they will show non-reciprocal response or not. This research may also be extended to investigation of surface wave propagation in films with patterned thickness and examination of their non-reciprocal response.

Future extension of this study may include exploration of inertia effects and dynamic peeling, studying the effect of different thickness profiles on the peeling response, and optimizing the film shape for the highest possible asymmetry ratio. It may also include investigating the effect of patterning thickness on peeling of 2D sheets.

4. METHODS

4.1 Analytical Solution: The solution Scheme

We follow the analytical procedure developed by Xia et al. [16] for the analysis of adhesion in heterogeneous thin film. The strip is being peeled by a force $\boldsymbol{F}$ with peeling angle θ_p. The force $\boldsymbol{F}$ is given by:

$$\boldsymbol{F} = F\begin{pmatrix} cos\ \theta_p \\ sin\ \theta_p \end{pmatrix} \tag{6}$$

And the tip displacement $\boldsymbol{u_p}$ is given by:

$$\boldsymbol{u_p} = \int_0^{S_N} \begin{pmatrix} cos\ \theta - cos\ \theta_p \\ sin\ \theta - sin\ \theta_p \end{pmatrix} ds \tag{7}$$

which is measured relative to a reference position at $\begin{pmatrix} S_N\ cos\ \theta_p \\ S_N\ sin\ \theta_p \end{pmatrix}$. There are two boundary conditions:

$$\theta(l) = 0, \quad \theta'(S_N^-) = 0 \tag{8}$$

The second boundary condition is due to the absence of applied moment at S_N. The negative superscript denotes the limit from the left. The potential energy of the system is given by:

$$\varepsilon = \int_l^{S_N} \frac{1}{2} D(s)\big(\theta'(s)\big)^2 ds - \boldsymbol{F}.\boldsymbol{u_p} - \int_0^l G ds \tag{9}$$

Where G is the adhesion energy per unit length of the interface between the strip and the substrate. We assume that both the material and the adhesive are rate-independent at low peeling velocities. In addition, we assume a smooth homogenous interface, and thus take G as a constant value. Substituting **Eq. 6, 7**, and assuming a constant bending rigidity within each discretized segment $D(s) = D_i(s_{i-1} < s < s_{i+1})$, the potential energy reduces to **Eq. 1**.

The condition for equilibrium is that the first variation of this equation with respect to θ and l should vanish for any values of $\delta\theta$ and δl consistent with the boundary conditions. Making use of this and the slope continuity at each discretization point $\theta(S_i^-) = \theta(S_i^+),\ 1 \le i \le N-1$, **Eq. 2, 3** are obtained. The detailed derivation is shown in Xia et al. [16].

Equations 2, 3 are solved numerically to determine the $(N+1)$ unknowns (the force F and the slope angles $\theta_1 : \theta_N$). The solution scheme is as follows:

1. For a given peel front position $\boldsymbol{s}$, where $\boldsymbol{s} = [s_1\ s_2\ \ldots\ldots s_N]$, and the segments rigidity $\boldsymbol{D} = [D_1\ D_2\ \ldots\ldots D_N]$, make an initial guess for $\boldsymbol{\theta} = [\theta_1\ \theta_2\ \ldots\ldots \theta_N]$.
2. Calculate F from **Eq. 2** using the current $\boldsymbol{\theta}$.

3. For $k = 1$ to N, calculate θ_k from θ_{k-1} using **Eq. 3**. We have chosen trapezoid method for solving the initial value problem where $\theta_o = 0$, and:

$$\theta_k = \theta_{k-1} + \frac{1}{2}\left(\frac{d\theta}{ds}(\theta_k) + \frac{d\theta}{ds}(\theta_{k-1})\right)(S_k - S_{k-1}) \tag{10}$$

   This is a nonlinear equation that is solved for θ_k.

4. Recalculate F using the updated $\boldsymbol{\theta}$.

5. Check the relative error between the previous and the updated value of F. If the error is greater than a defined tolerance, go to step 3. Otherwise, go to step 6. The tolerance is set to 10^{-5}.

6. Calculate the tip displacement for the current peel front position. Advance the peel front position and repeat.

We have discretized every unit cell into a large enough number of segments to ensure that the linearly varying strip thickness is accurately approximated by a series of constant thickness intervals. We have chosen the segment width to be at least $p/100$ where p is the width of the periodic unit cell of the strip. Further mesh refinement has negligible effect on the solution.

4.2 Finite Element Analysis: Model Setup

We use the finite element software package ABAQUS [28]. The model setup is shown in **Fig. 5.** We conduct Implicit dynamic analysis with slow peeling rate to represent a quasi-static peeling test under displacement-controlled boundary conditions without considering gravity loads. The dimensions of the base plate are chosen in a way that the boundaries have no effect on the results. The lower edge of the base plate is

restrained from movement in both directions. The base plate is tilted to have an angle of θ_p with the vertical upward direction. The edge of the strip is pulled upwards with a constant rate.

To model the cohesive interface, we implement a zero-thickness cohesive element. We adopt an intrinsic bilinear cohesive law composed of a linear elastic part up to the critical cohesive stress σ_{cr}, followed by linear degradation that evolves from crack initiation to complete failure. The analytical expression for the cohesive law is given by:

$$\sigma(\Delta) = \begin{cases} K_o\Delta, & \Delta \le \gamma\Delta_f \\ \sigma_{cr}(\Delta_f - \Delta)/(\Delta_f - \gamma\Delta_f), & \gamma\Delta_f \le \Delta \le \Delta_f \\ 0, & \Delta \ge \Delta_f \end{cases} \quad (11)$$

Where K_o is penalty stiffness of the cohesive law, Δ_f is the failure (total separation) normal displacement, and γ is the ratio between the critical and the failure normal displacements. K_o value may be determined by selecting proper values of σ_{cr} and γ. The total area under the curve is the cohesive fracture energy G_c, and the length on which stress changes from σ_{cr} (Crack initiation) to 0 (total separation) defines the cohesive zone length l.

We have chosen the strip longitudinal dimension to have at least 10 periods, and all results are obtained after reaching steady state peeling. The strip is meshed using 2D plane strain quadrilateral elements and the cohesive interface is meshed using zero thickness cohesive elements. The cohesive elements size is chosen to be $L_{pz}/100$ at

most to avoid solution jump that may result in divergence or global oscillations [42]. We have conducted a mesh sensitivity analysis to insure adequate accuracy.

FUNDING

This research has been supported by funds from Campus Research Board of University of Illinois Urbana Champaign (RB17043), and the National Science Foundation grants (CMMI-Award Number 1435920) and (CAREER Award Number 1753249).

REFERENCES

[1] C. H. Lee, D. R. Kim, I. S. Cho, N. William, Q. Wang, and X. Zheng, "Peel-and-stick: Fabricating thin film solar cell on universal substrates," *Sci. Rep.*, vol. 2, no. January 2014, 2012.

[2] P. G. and Q. Zhang, "Encapsulate-and-peel: fabricating carbon nanotube CMOS integrated circuits in a flexible ultra-thin plastic film," *Nanotechnology*, vol. 25, no. 6, p. 65301, 2014.

[3] C. H. Lee, J. H. Kim, C. Zou, I. S. Cho, J. M. Weisse, W. Nemeth, Q. Wang, A. C. T. Van Duin, T. S. Kim, and X. Zheng, "Peel-And-stick: Mechanism study for efficient fabrication of flexible/ transparent thin-film electronics," *Sci. Rep.*, vol. 3, pp. 1–6, 2013.

[4] C. Kovalchick, A. Molinari, and G. Ravichandran, "Rate Dependent Adhesion Energy and Nonsteady Peeling of Inextensible Tapes," *J. Appl. Mech.*, vol. 81, no. 4, p. 041016, 2013.

[5] I. L. Singer, J. G. Kohl, and M. Patterson, "Mechanical aspects of silicone coatings for hard foulant control," *Biofouling*, vol. 16, no. 2–4, pp. 301–309, 2000.

[6] B. Laulicht, R. Langer, and J. M. Karp, "Quick-release medical tape," *Proc. Natl. Acad. Sci.*, vol. 109, no. 46, pp. 18803–18808, 2012.

[7] Rivlin R. S., "The Effective work of adhesion Experiments with Adhesive Tape," *Paint Technol.*, vol. IX, no. 106, pp. 2611–2614, 1944.

[8] S. Kim, J. Wu, A. Carlson, S. H. Jin, A. Kovalsky, P. Glass, Z. Liu, N. Ahmed, S. L. Elgan, W. Chen, P. M. Ferreira, M. Sitti, Y. Huang, and J. A. Rogers, "Microstructured elastomeric surfaces with reversible adhesion and examples of their use in deterministic assembly by transfer printing," *Proc. Natl. Acad. Sci.*, vol. 107, no. 40, pp. 17095–17100, 2010.

[9] K. Kendall, "Thin-Film Peeling - The Elastic Term," *J. Phys. D. Appl. Phys.*, vol. 8, pp. 1449–1452, 1975.

[10] A. G. Evans and J. W. Hutchinson, "Effects of non-planarity on the mixed mode fracture resistance of bimaterial interfaces," *Acta Metall.*, vol. 37, no. 3, pp. 909–916, 1989.

[11] P. R. Guduru and C. Bull, "Detachment of a rigid solid from an elastic wavy surface: Experiments," *J. Mech. Phys. Solids*, vol. 55, no. 3, pp. 473–488, 2007.

[12] Q. Li and K. S. Kim, "Micromechanics of rough surface adhesion: a homogenized projection method," *Acta Mech. Solida Sin.*, vol. 22, no. 5, pp. 377–390, 2009.

[13] L. Brely, F. Bosia, and N. M. Pugno, "The influence of substrate roughness, patterning, curvature, and compliance in peeling problems," *Bioinspiration and Biomimetics*, vol. 13, no. 2, p. aaa0e5, 2018.

[14] K. Kendall, "Control of Cracks by Interfaces in Composites," *Proc. R. Soc. A*

Math. Phys. Eng. Sci., vol. 341, no. 1627, pp. 409–428, 1975.

[15] A. Ghatak, L. Mahadevan, J. Y. Chung, M. K. Chaudhury, and V. Shenoy, "Peeling from a biomimetically patterned thin elastic film," *Proc. R. Soc. London. Ser. A Math. Phys. Eng. Sci.*, vol. 460, no. 2049, p. 2725 LP-2735, Sep. 2004.

[16] S. M. Xia, L. Ponson, G. Ravichandran, and K. Bhattacharya, "Adhesion of heterogeneous thin films - I: Elastic heterogeneity," *J. Mech. Phys. Solids*, vol. 61, no. 3, pp. 838–851, 2013.

[17] S. Xia, L. Ponson, G. Ravichandran, and K. Bhattacharya, "Toughening and asymmetry in peeling of heterogeneous adhesives," *Phys. Rev. Lett.*, vol. 108, no. 19, pp. 1–5, 2012.

[18] S. M. Xia, L. Ponson, G. Ravichandran, and K. Bhattacharya, "Adhesion of heterogeneous thin films II: Adhesive heterogeneity," *J. Mech. Phys. Solids*, vol. 83, pp. 88–103, 2015.

[19] J. D. Reedy, "Effects of patterned nanoscale interfacial roughness on interfacial toughness: A finite element analysis," *J. Mater. Res.*, vol. 23, no. 11, pp. 3056–3065, 2008.

[20] H.-P. ZHAO, Y. WANG, B.-W. LI, and X.-Q. FENG, "Improvement of the Peeling Strength of Thin Films By a Bioinspired Hierarchical Interface," *Int. J. Appl. Mech.*, vol. 05, no. 02, p. 1350012, 2013.

[21] D. G. Hwang, K. Trent, and M. D. Bartlett, "Kirigami-Inspired Structures for Smart Adhesion," *ACS Appl. Mater. Interfaces*, vol. 10, no. 7, pp. 6747–6754, 2018.

[22] C.-J. Hsueh and K. Bhattacharya, "Optimizing microstructure for toughness : the model problem of peeling," 2018.

[23] D. Santos, M. Spenko, A. Parness, S. Kim, and M. Cutkosky, "Directional adhesion for climbing: theoretical and practical considerations," *J. Adhes. Sci. Technol.*, vol. 21, no. 12–13, pp. 1317–1341, Jan. 2007.

[24] H. Lee, B. P. Lee, and P. B. Messersmith, "A reversible wet/dry adhesive inspired by mussels and geckos," *Nature*, vol. 448, no. 7151, pp. 338–341, 2007.

[25] K. Autumn, "Gecko Adhesion: Structure, Function, and Applications Kellar," vol. 32, no. June, pp. 473–478, 2007.

[26] J. Y. Chung and M. K. Chaudhury, "Bio-inspired Duplex Attachment Pad with Asymmetric Adhesion," in *Biological and Biomimetic Adhesives: Challenges and Opportunities*, The Royal Society of Chemistry, 2013, pp. 72–85.

[27] J. Seo, J. Eisenhaure, and S. Kim, "Micro-wedge array surface of a shape memory polymer as a reversible dry adhesive," *Extrem. Mech. Lett.*, vol. 9, pp. 207–214, 2016.

[28] "Abaqus Analysis User's Manual, 6.13th ed." Dassault Systemes Simulia Corp.,

Providence, RI, USA, 2013.

[29] J. G. Williams and H. Hadavinia, "Analytical solutions for cohesive zone models," *J. Mech. Phys. Solids*, vol. 50, no. 4, pp. 809–825, 2002.

[30] K. Ha, H. Baek, and K. Park, "Convergence of fracture process zone size in cohesive zone modeling," *Appl. Math. Model.*, vol. 39, no. 19, pp. 5828–5836, 2015.

[31] D. Adams and L. a. C. R. B. Pipes, *Experimental characterization of advanced composite materials*. 2003.

[32] P. Qiao, J. Wang, and J. F. Davalos, *Tapered beam on elastic foundation model for compliance rate change of TDCB specimen*, vol. 70, no. 2. 2003.

[33] L. Avellar, T. Reese, K. Bhattacharya, and G. Ravichandran, "Effect of cohesive zone size on peeling of heterogeneous adhesive tape," *J. Appl. Mech.*, no. c, 2018.

[34] J. D. Eisenhaure, T. Xie, S. Varghese, and S. Kim, "Microstructured shape memory polymer surfaces with reversible dry adhesion," *ACS Appl. Mater. Interfaces*, vol. 5, no. 16, pp. 7714–7717, 2013.

[35] M. Geissler and Y. Xia, "Patterning: Principles and some new developments," *Adv. Mater.*, vol. 16, no. 15 SPEC. ISS., pp. 1249–1269, 2004.

[36] M. Z. Hossain, C. J. Hsueh, B. Bourdin, and K. Bhattacharya, "Effective toughness of heterogeneous media," *J. Mech. Phys. Solids*, vol. 71, no. 1, pp. 15–32, 2014.

[37] Q. Chen and A. Elbanna, "Emergent wave phenomena in coupled elastic bars: From extreme attenuation to realization of elastodynamic switches," *Sci. Rep.*, vol. 7, no. 1, p. 16204, 2017.

[38] M. Taylor, L. Francesconi, M. Gerendás, A. Shanian, C. Carson, and K. Bertoldi, "Low porosity metallic periodic structures with negative poisson's ratio," *Adv. Mater.*, vol. 26, no. 15, pp. 2365–2370, 2014.

[39] A. Ghareeb and A. Elbanna, "On the Role of the Plaque Porous Structure in Mussel Adhesion: Implications for Adhesion Control Using Bulk Patterning," *J. Appl. Mech.*, vol. 85, no. 12, p. 121003, 2018.

[40] A. Ghareeb and A. Elbanna, "Extreme Enhancement of Interfacial Adhesion by Bulk Patterning of Sacrificial Cuts Ahmed Ghareeb," *Extrem. Mech. Lett.*, vol. 28, pp. 22–30, 2019.

[41] G. Trainiti and M. Ruzzene, "Non-Reciprocal Wave Propagation in Spatiotemporal Periodic Structures," 2016.

[42] A. Turon, C. G. Dávila, P. P. Camanho, and J. Costa, "An engineering solution for mesh size effects in the simulation of delamination using cohesive zone models," *Eng. Fract. Mech.*, vol. 74, no. 10, pp. 1665–1682, 2007.

Figure Captions List

Fig. 1 Peeling of a thin strip with patterned thickness from a rigid substrate: (a) Idealized longitudinal profile of the strip modeled as an Euler-Bernoulli beam, and (b) the thin strip profile showing the actual thickness of the strip, and (c) representation of the strip profile based on the effective thickness concept allowing for a gradual redistribution of the bending stresses over a transition length at locations of step change in thickness. The forward and backward peeling directions are also highlighted.

Fig. 2 Comparison between the theoretical models and finite element results: (a), (b) the normalized forces vs. normalized peel front position for forward and backward peeling directions, $t_l/t_h = 0.5, p/\lambda = 3.33$. (c), (d) the normalized forces vs. normalized vertical peel displacement for forward and backward peeling directions, $t_l/t_h = 0.5, p/\lambda = 3.33$. The hatched areas represent the energy dissipated due to the snap-back instability. (e), (f) the normalized peak forces vs. p/λ for forward and backward peeling and $t_l/t_h = 0.50$.

Fig. 3 Dependence of peeling force and adhesion asymmetry on different model parameters: (a), (b) Effect of the ratio of minimum to maximum thicknesses of the strip on the normalized peak forces and the asymmetry ratio for different values of period length for both peeling directions. The asymmetry ratio increases as the thickness ratio

decreases and the period length increases. (c), (d) Effect of the ratio of period to the length scale of the bending on the normalized peak forces and the asymmetry ratio for two values of thickness ratio and both peeling directions. The peak force for peeling in the forward direction monotonically increases as the normalized period increases. The peak force for peeling in the backward direction shows a non-monotonic dependence on the normalized period. The asymmetry ratio increases with the increase in the normalized period. (e), (f) Effect of the ratio of cohesive law characteristic length to the length scale of the bending on the normalized peak forces and the asymmetry ratio for $t_l/t_h = 0.125$, $p/\lambda = 5$ for both peeling directions. The normalized peak force significantly decreases in forward peeling direction as the cohesive length scale increases relative to the length scale of bending. The asymmetry ratio increases, and approaches its theoretical limit, as the cohesive length scale decreases relative to the length scale of the bending. The results in this figure are obtained using the finite element model unless otherwise mentioned.

Fig. 4 Change in strain energy at steady state peeling: The normalized strain energy of the strip vs. the normalized peel front location for both forward and backward propagation, $t_l/t_h = 0.25$, and $p/\lambda = 3.33$. The results in this figure are obtained using the finite element model.

Fig. 5 Model setup for the finite element analysis. A homogenous thin film with saw tooth thickness profile is peeled from a rigid substrate. The peeling angle is θ_p.

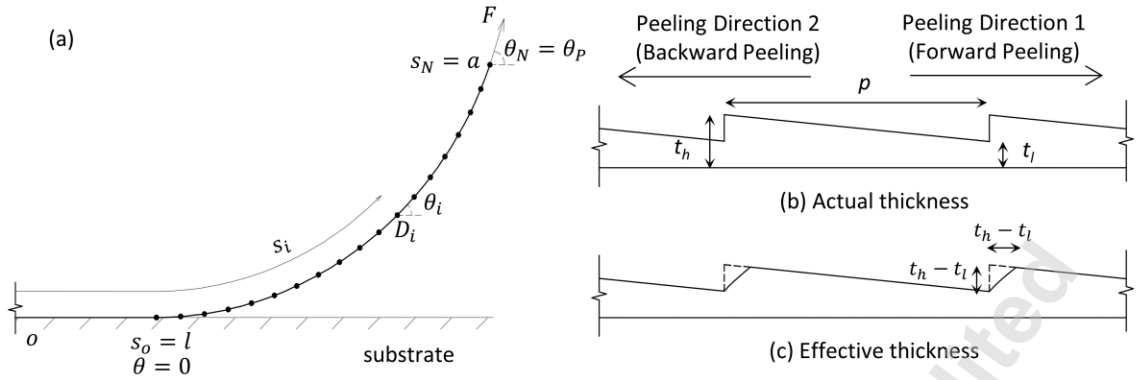

Fig. 1: Peeling of a thin strip with patterned thickness from a rigid substrate: (a) Idealized longitudinal profile of the strip modeled as an Euler-Bernoulli beam, and (b) the thin strip profile showing the actual thickness of the strip, and (c) representation of the strip profile based on the effective thickness concept allowing for a gradual redistribution of the bending stresses over a transition length at locations of step change in thickness. The forward and backward peeling directions are also highlighted.

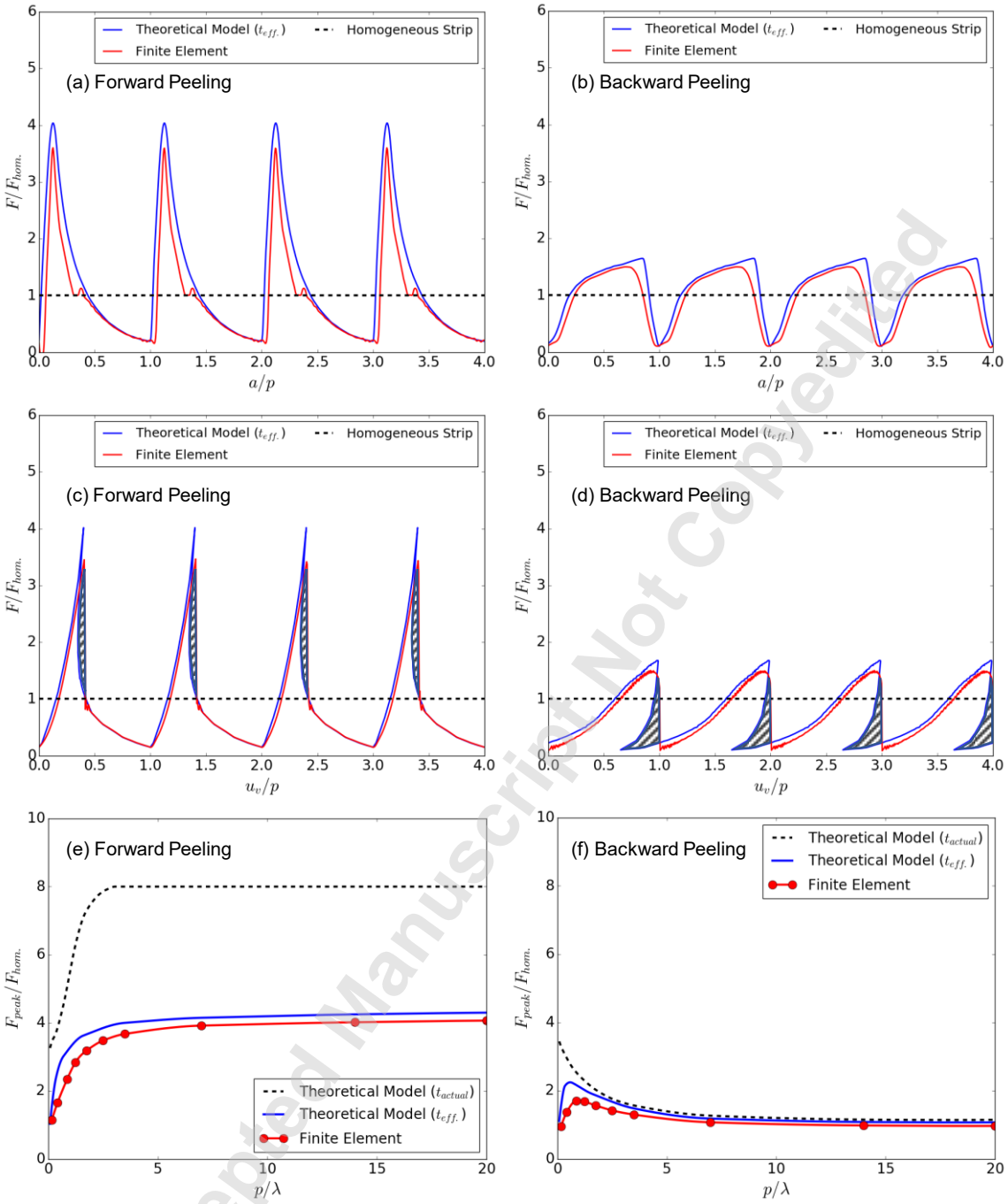

Fig. 2: Comparison between the theoretical models and finite element results: (a), (b) the normalized forces vs. normalized peel front position for forward and backward peeling directions, $t_l/t_h = 0.5$, $p/\lambda = 3.33$. (c), (d) the normalized forces vs. normalized vertical peel displacement for forward and backward peeling directions, $t_l/t_h = 0.5$,

$p/\lambda = 3.33$. The hatched areas represent the energy dissipated due to the snap-back instability. (e), (f) the normalized peak forces vs. p/λ for forward and backward peeling and $t_l/t_h = 0.50$.

Journal of Applied Mechanics. Received January 28, 2019;
Accepted manuscript posted March 24, 2019. doi:10.1115/1.4043286

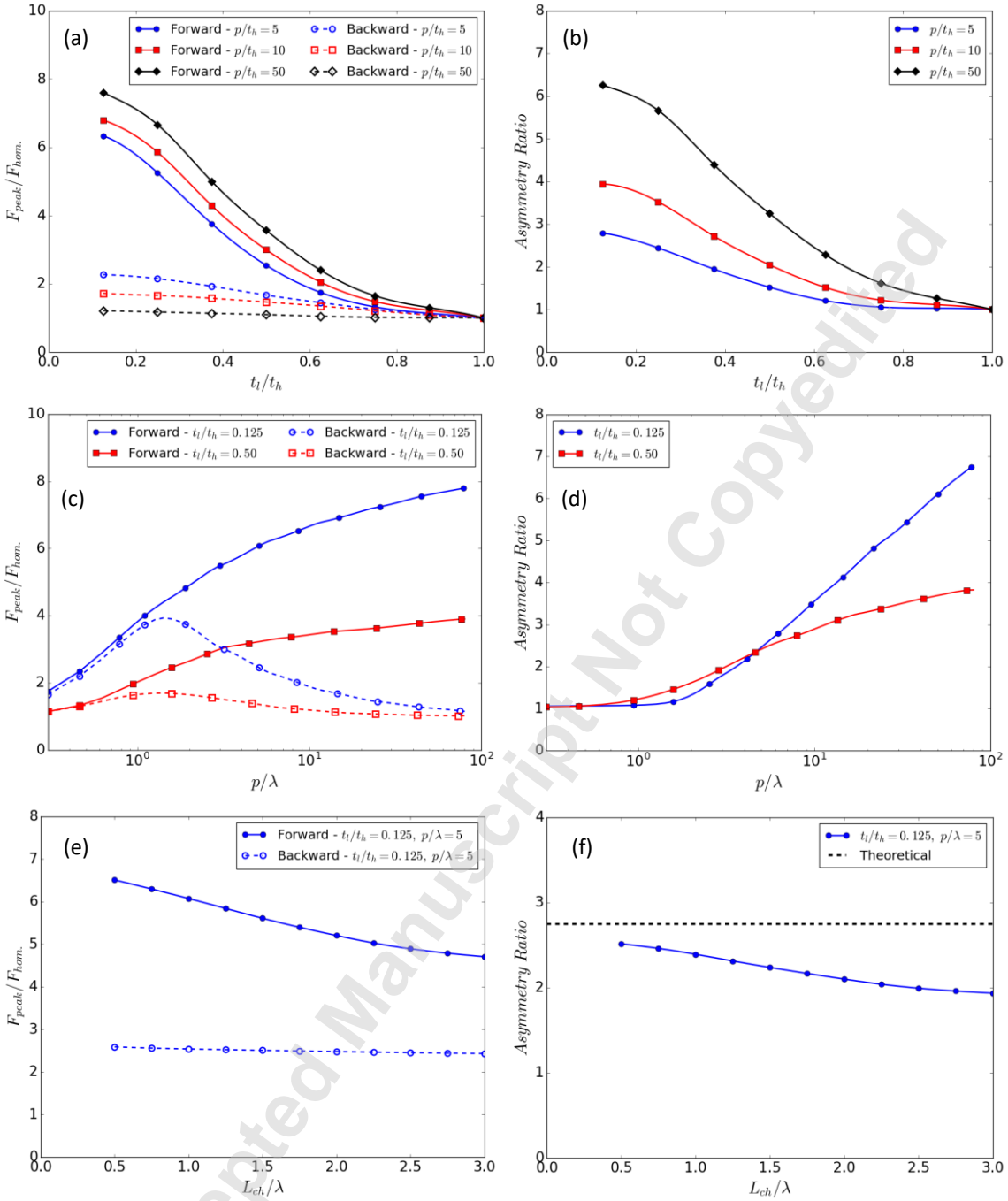

Fig. 3: Dependence of peeling force and adhesion asymmetry on different model parameters: (a), (b) Effect of the ratio of minimum to maximum thicknesses of the strip on the normalized peak forces and the asymmetry ratio for different values of period length for both peeling directions. The asymmetry ratio increases as the thickness ratio

decreases and the period length increases. (c), (d) Effect of the ratio of period to the length scale of the bending on the normalized peak forces and the asymmetry ratio for two values of thickness ratio and both peeling directions. The peak force for peeling in the forward direction monotonically increases as the normalized period increases. The peak force for peeling in the backward direction shows a non-monotonic dependence on the normalized period. The asymmetry ratio increases with the increase in the normalized period. (e), (f) Effect of the ratio of cohesive law characteristic length to the length scale of the bending on the normalized peak forces and the asymmetry ratio for $t_l/t_h = 0.125$, $p/\lambda = 5$ for both peeling directions. The normalized peak force significantly decreases in forward peeling direction as the cohesive length scale increases relative to the length scale of bending. The asymmetry ratio increases, and approaches its theoretical limit, as the cohesive length scale decreases relative to the length scale of the bending. The results in this figure are obtained using the finite element model unless otherwise mentioned.

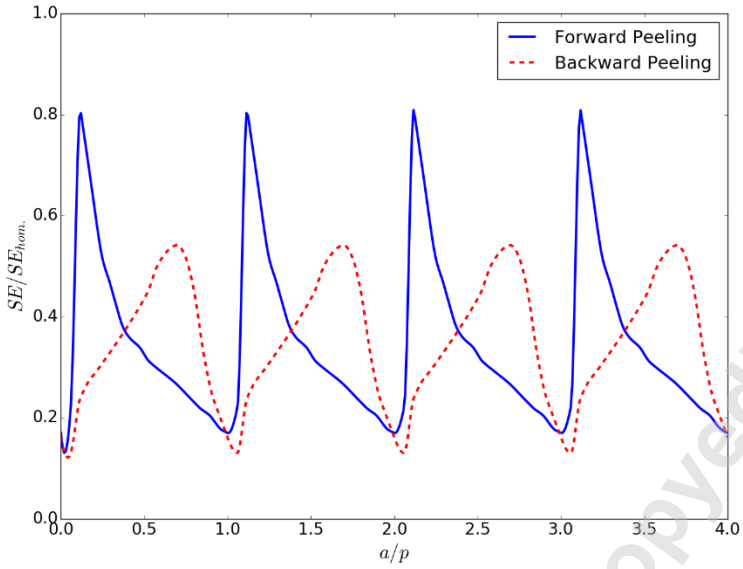

Fig. 4: Change in strain energy at steady state peeling: The normalized strain energy of the strip vs. the normalized peel front location for both forward and backward propagation, $t_l/t_h = 0.25$, and $p/\lambda = 3.33$. The results in this figure are obtained using the finite element model.

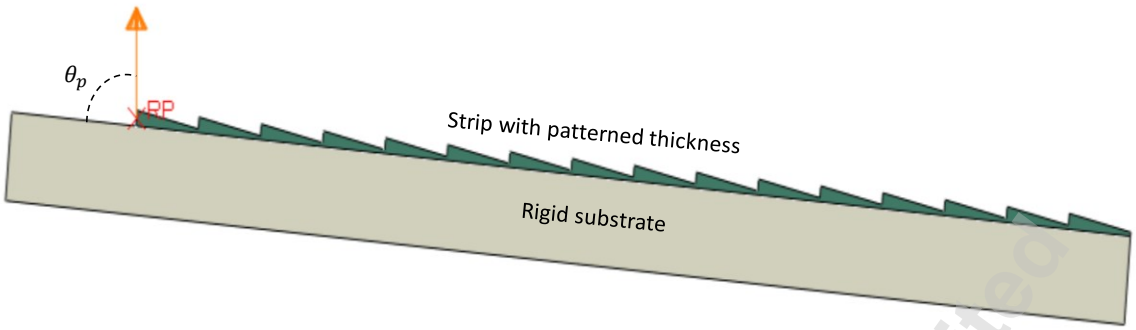

Fig. 5: Model setup for the finite element analysis. A homogenous thin film with saw tooth thickness profile is peeled from a rigid substrate. The peeling angle is θ_p.